Supporting Information

Characterizing Residue-Bilayer Interactions Using Gramicidin A as a Scaffold and Tryptophan Substitutions as Probes

Andrew H. Beaven, Alexander J. Sodt, Richard W. Pastor, Roger E. Koeppe II, Olaf S. Andersen, Wonpil Im

Table S1. System information. All systems have 90 lipids / leaflet. A "d" denotes a dimer simulation and an "m" denotes a monomer simulation. The gA^{Trp} simulations in $dC_{20:1}$ and $dC_{22:1}$ are taken from Sodt et al.[1]

Mutant	Lipid Type	ID	System Size[$]	Water	Total Atoms	Sim. Time [ns]
gA^{Trp} d	$dC_{18:1}$	1	79.7×79.7×70.0	6,802	45,835	220
		2	79.7×79.7×70.0	6,756	45,697	220
		3	79.7×79.7×70.0	6,743	45,658	220
	$dC_{20:1}$	1	80.0×80.0×86.0	8,148	52,050	110
	$dC_{22:1}$	1	80.0×80.0×87.0	8,063	53,957	110
gA^{Trp} m	$dC_{20:1}$	1	79.3×79.3×88.0	8,119	51,965	110
	$dC_{22:1}$	1	79.2×79.2×90.0	8,194	54,352	110
gA^{mTrp} d	$dC_{18:1}$	1	79.8×79.8×80.0	8,928	52,249	220
		2	79.8×79.8×80.0	9,000	52,465	220
		3	79.8×79.8×80.0	8,870	52,075	220
	$dC_{20:1}$	1	80.0×80.0×86.0	7,789	50,997	140
		2	80.0×80.0×86.0	7,774	50,952	170
		3	80.0×80.0×86.0	7,796	51,018	130
	$dC_{22:1}$	1	80.0×80.0×87.0	7,775	53,117	130
		2	80.0×80.0×87.0	7,789	53,159	130
		3	80.0×80.0×87.0	7,803	53,201	130
gA^{mTrp} m	$dC_{20:1}$	1	79.4×79.4×88.0	8,164	52,124	150
		2	79.4×79.4×88.0	8,170	52,142	130
		3	79.4×79.4×88.0	8,160	52,112	80
	$dC_{22:1}$	1	79.3×79.3×90.0	8,241	54,517	130
		2	79.3×79.3×90.0	8,217	54,445	130
		3	79.3×79.3×90.0	8,196	54,382	130
$gA^{nc\text{-}mTrp}$ d	$dC_{18:1}$	1	79.8×79.8×80.0	8,917	52,216	220
		2	79.8×79.8×80.0	8,887	52,126	220
		3	79.8×79.8×80.0	8,870	52,075	220
	$dC_{20:1}$	1	79.4×79.4×86.0	7,708	50,754	100
		2	79.4×79.4×86.0	7,689	50,697	100
		3	79.4×79.4×86.0	7,683	50,679	100
	$dC_{22:1}$	1	79.3×79.3×87.0	7,634	52,692	100
		2	79.3×79.3×87.0	7,651	52,743	100
		3	79.3×79.3×87.0	7,656	52,758	100
$gA^{nc\text{-}mTrp}$ m	$dC_{20:1}$	1	79.4×79.4×88.0	8,172	52,148	100
		2	79.4×79.4×88.0	8,170	52,142	100
		3	79.4×79.4×88.0	8,181	52,175	100
	$dC_{22:1}$	1	79.3×79.3×90.0	8,205	54,409	100
		2	79.3×79.3×90.0	8,216	54,442	100
		3	79.3×79.3×90.0	8,241	54,517	100

gA^{Tyr} d	$dC_{18:1}$	1	79.5×79.5×80.0	8,893	52,094	220
		2	79.5×79.5×80.0	8,835	51,920	220
		3	79.5×79.5×80.0	8,927	52,196	220
	$dC_{22:1}$	1	79.0x79.0x87.0	7,554	52,404	100
		2	79.0x79.0x87.0	7,568	52,446	100
		3	79.0x79.0x87.0	7,544	52,374	100
gA^{Tyr} m	$dC_{22:1}$	1	79.0x79.0x90.0	8,208	54,370	100
		2	79.0x79.0x90.0	8,208	54,370	100
		3	79.0x79.0x90.0	8,208	54,370	100
gA^{Phe} d	$dC_{18:1}$	1	79.5×79.5×80.0	8,889	52,074	220
		2	79.5×79.5×80.0	8,852	51,963	220
		3	79.5×79.5×80.0	8,852	51,963	220
	$dC_{22:1}$	1	79.0x79.0x87.0	7,541	52,357	100
		2	79.0x79.0x87.0	7,528	52,318	100
		3	79.0x79.0x87.0	7,545	52,370	100
gA^{Phe} m	$dC_{22:1}$	1	79.0x79.0x90.0	8,161	54,221	100
		2	79.0x79.0x90.0	8,149	54,185	100
		3	79.0x79.0x90.0	8,112	54,075	100
gA^{Gln} d	$dC_{18:1}$	1	79.4×79.4×80.0	8,856	51,951	220
		2	79.4×79.4×80.0	8,827	51,864	220
		3	79.4×79.4×80.0	8,845	51,918	220
gA^{Leu} d	$dC_{18:1}$	1	79.4×79.4×80.0	8,818	51,853	220
		2	79.4×79.4×80.0	8,832	51,895	220
		3	79.4×79.4×80.0	8,834	51,901	220

Table S2. Average channel tilt angles (mean ± standard error). Channels with residues (at positions 9, 11, 13 an 15) that can hydrogen bond have less tilt.

Channel	Tilt Angle [°]
gA^{Trp}	9.3 ± 0.7
gA^{mTrp}	12.4 ± 0.3
$gA^{nc\text{-}mTrp}$	15.2 ± 0.9
gA^{Tyr}	12.2 ± 0.8
gA^{Phe}	13.8 ± 0.4
gA^{Gln}	10.9 ± 1.3
gA^{Leu}	15.0 ± 1.7

Table S3. Average count of phospholipid choline nitrogen atoms within r = 3 Å of the center of the channel pore (where they would block ion permeation). The channel's pore is aligned with the z-axis ($xy = 0$) and the number of choline N is counted as a function of time. The presented value provides the time-averaged fraction of choline N in the vicinity of the pore. Residues that cannot hydrogen bond, and therefore impose fewer constraints on the lipids adjacent to the channel) increase the probability of finding a choline N near the pore.

Channel	Avg ± St Err
gA^{Trp}	0.12 ± 0.02
gA^{mTrp}	0.26 ± 0.03
$gA^{nc\text{-}mTrp}$	0.30 ± 0.02
gA^{Tyr}	0.14 ± 0.02
gA^{Phe}	0.27 ± 0.02
gA^{Gln}	0.14 ± 0.02
gA^{Leu}	0.29 ± 0.01

Figure S1. Previously published[2] (A) gA^{Trp} monomer pore formation in $dC_{12:0}$ (1,2-di-lauroyl-PC, DLPC) in the left panel and $dC_{14:0}$ (1,2-di-myristoyl-PC, DMPC) in the right panel. (B) Monolayer hydrophobic thickness profiles in $dC_{12:0}$, which show an asymmetry in monolayer deformations due to an asymmetric channel. Reprinted from Biophysical Journal, 102, T. Kim, K.I. Lee, P. Morris, R.W. Pastor, O.S. Andersen, and W. Im, Influence of Hydrophobic Mismatch on Structures and Dynamics of Gramicidin A and Lipid Bilayers, 1551–1560, 2012, with permission from Elsevier.

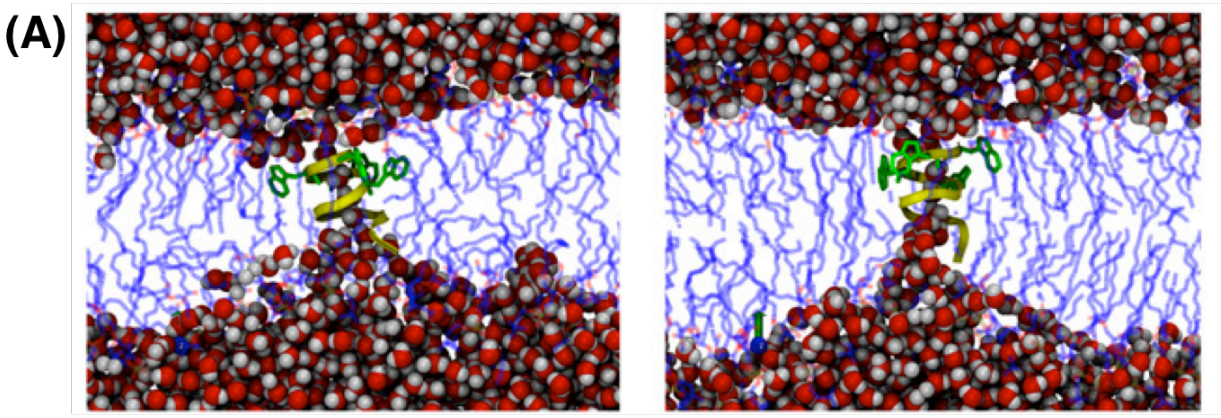

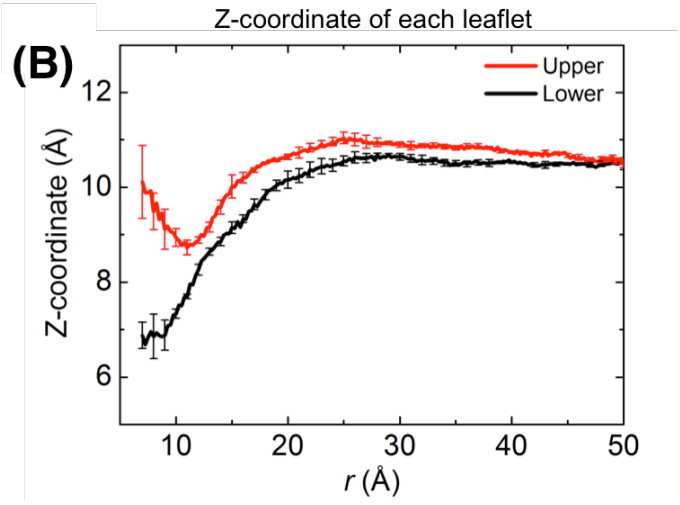

Figure S2. $dC_{22:1}$ lipid *sn-2* terminal carbon atom densities along the *z*-axis for both leaflets. The most populated *z* (for the bilayer) is at ~0 Å, but the unsigned weighted averages are at ~3.7 Å and ~3.3 Å for the upper and lower leaflets, respectively.

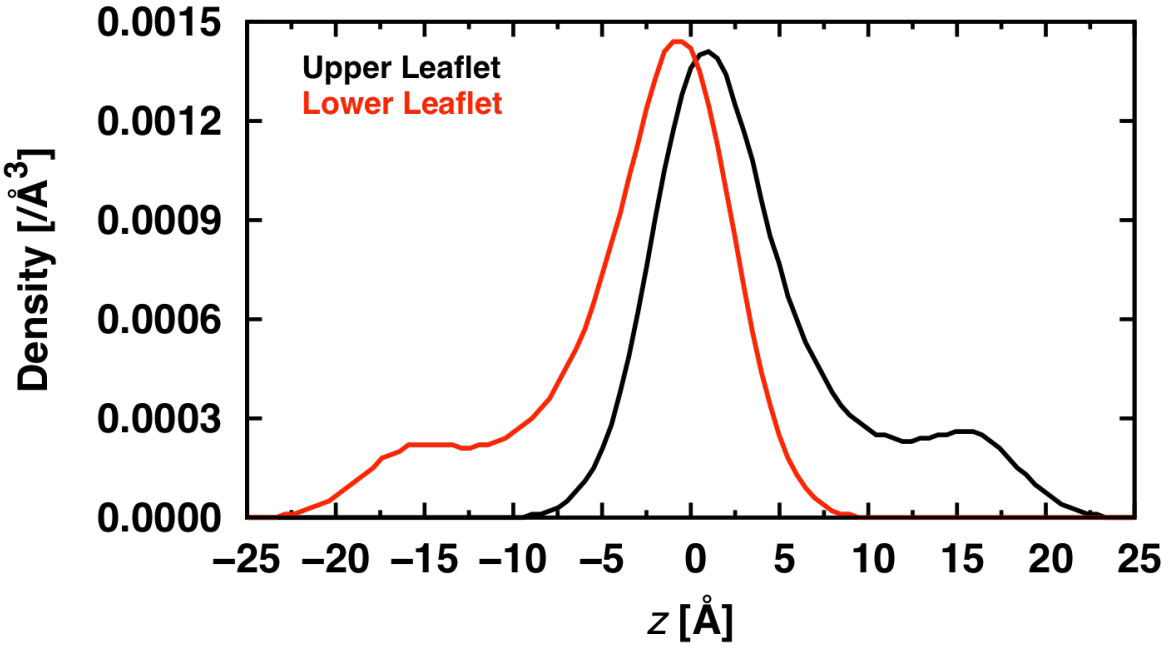

Figure S3. Heavy atom backbone root mean squared fluctuations (RMSF) for all channel types in $dC_{18:1}$. The "X" residues are those that were mutated, and "EA" is ethanolamide.

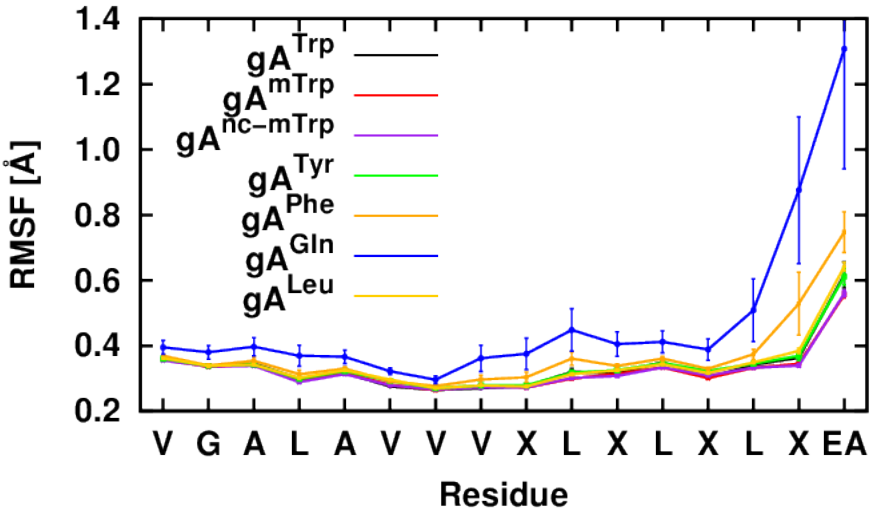

Figure S4. Time series of heavy atom backbone root mean square deviations (RMSD) for each channel type in $dC_{18:1}$ calculated relative to the minimized PDB:1JNO structure. Red, blue, and green are replicas 1, 2, and 3, respectively.

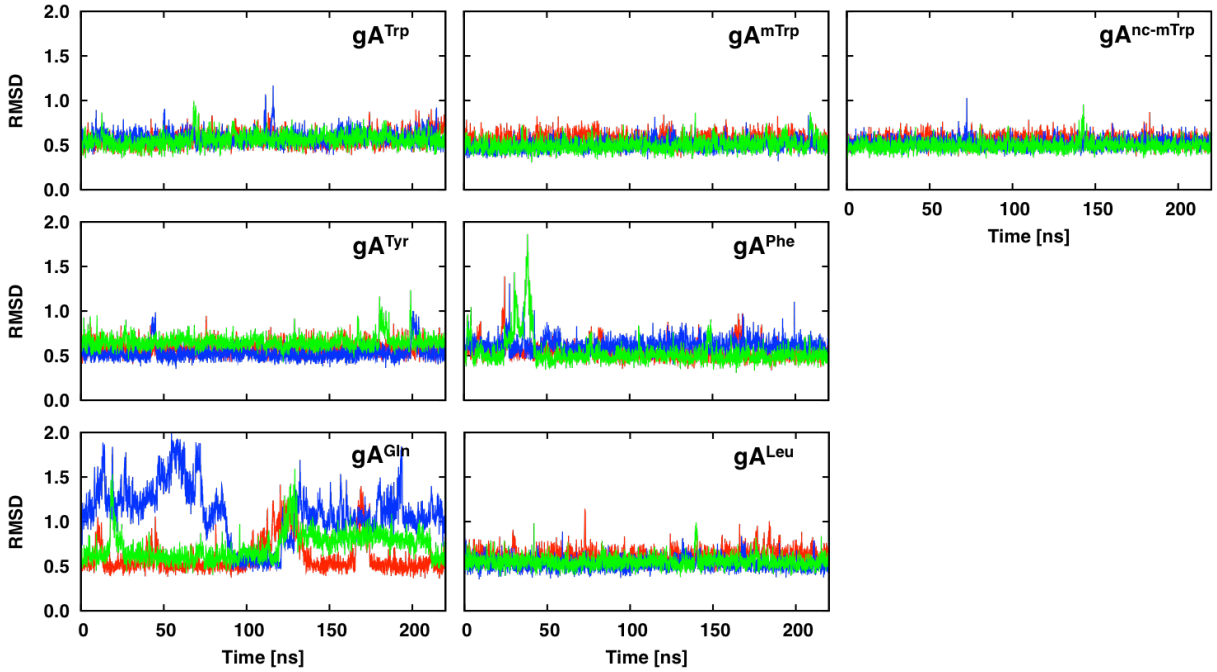

Figure S5. Channel tilt angle distributions for each channel type in $dC_{18:1}$ with 1° bin width. Area under each curve equals unity.

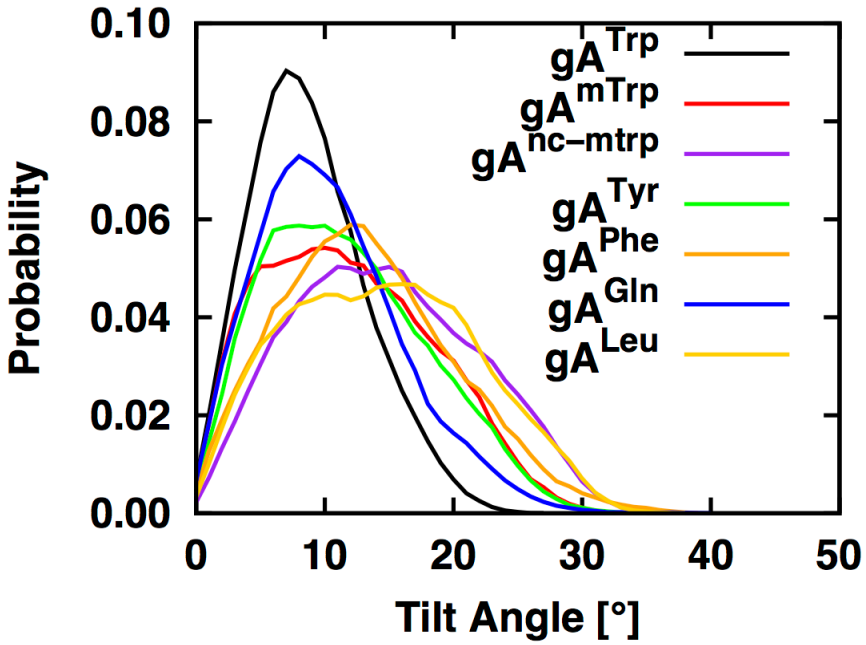

Figure S6. Tyr and Phe χ_1-χ_2 dihedral angles in $dC_{18:1}$. χ_1 is the dihedral of the backbone N, Cα, Cβ, and Cγ atoms. χ_2 is the dihedral of the Cα, Cβ, Cγ, and Cδ atoms. The color scheme for the heat plots is shown on the right with log{count/bin} and 1° bins in both dimensions.

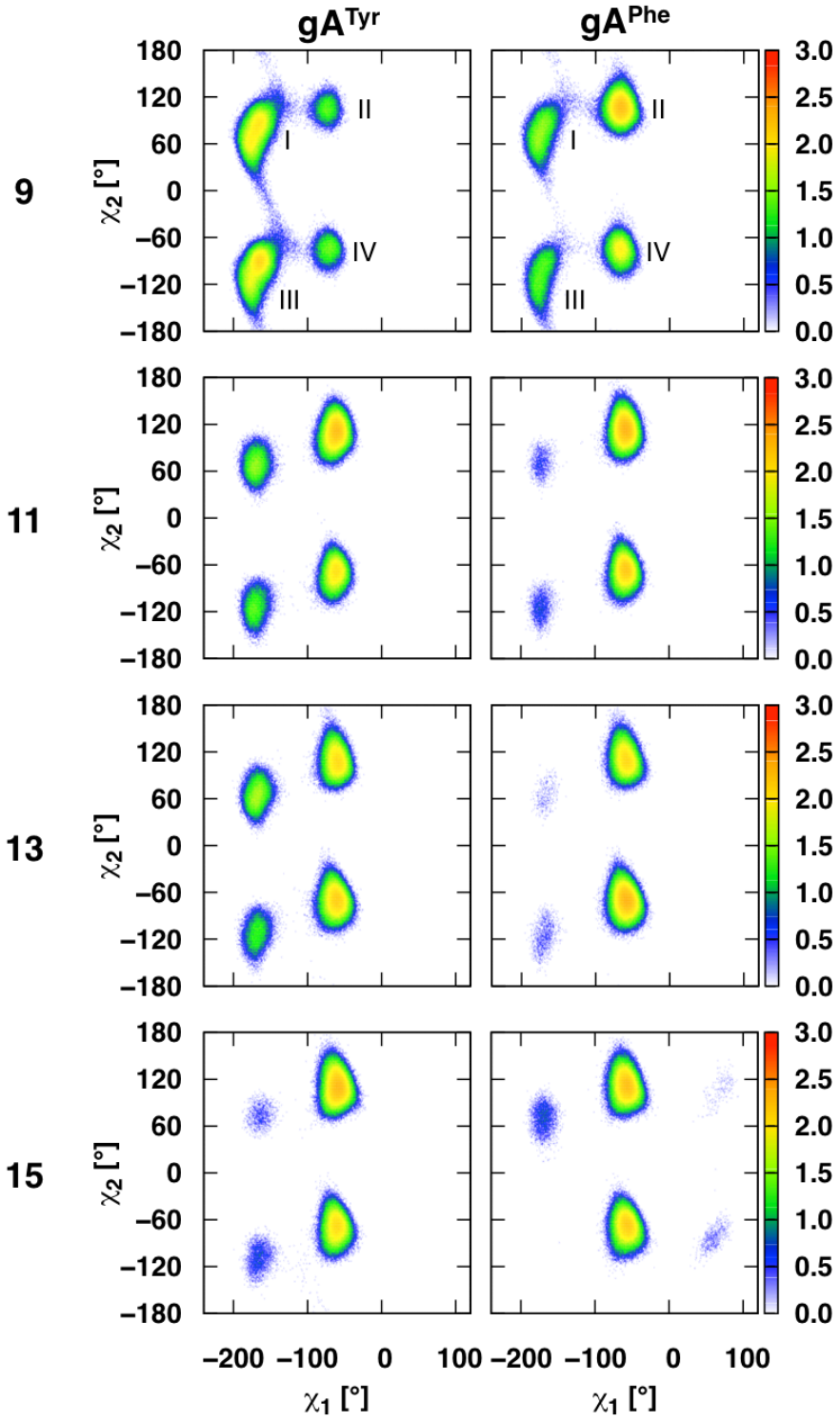

Figure S7. Gln and Leu χ_1-χ_2 dihedral angles in $dC_{18:1}$. See the **Figure S6** caption for the figure notation.

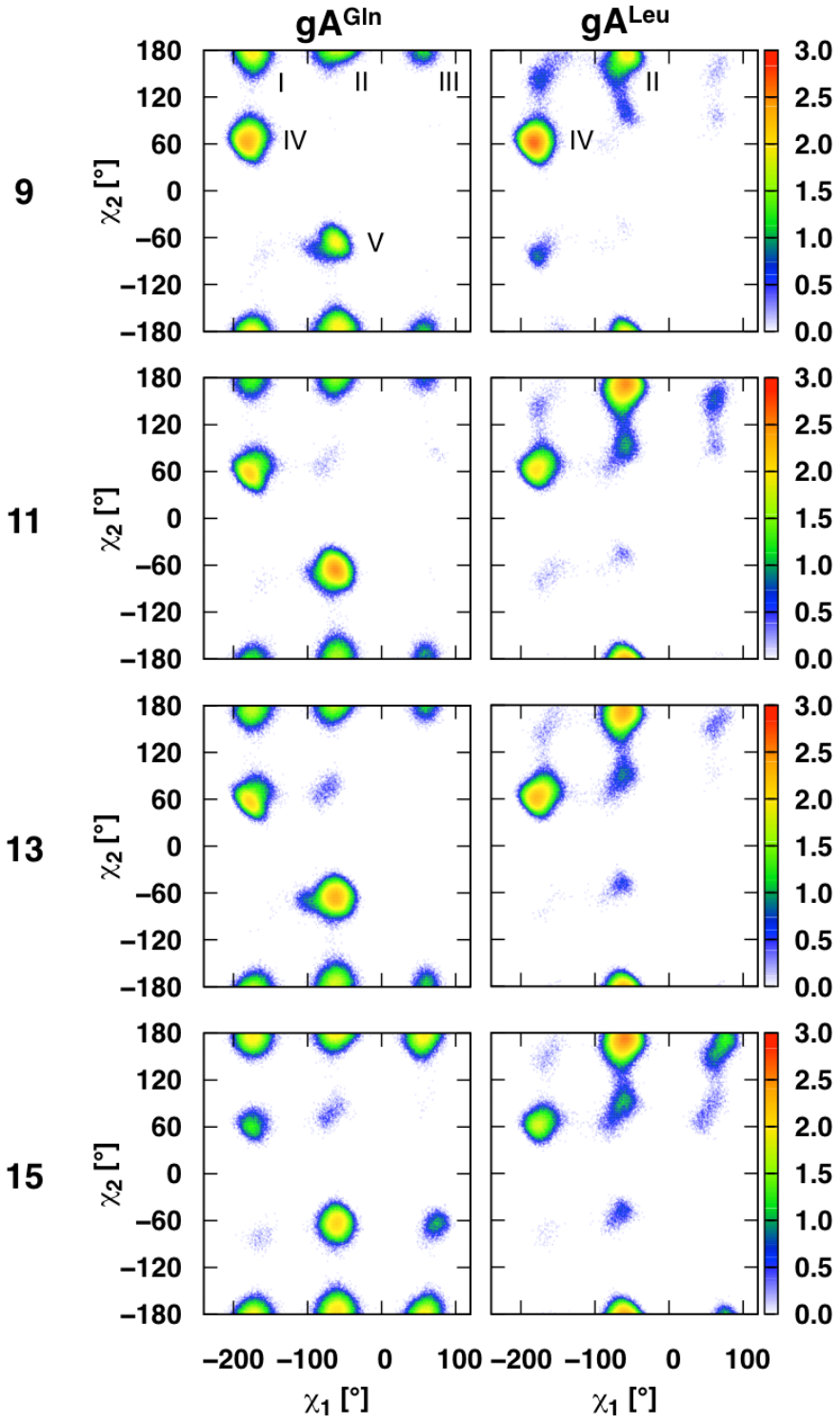

Figure S8. Radial distribution functions (RDFs) for $dC_{18:1}$ lipids around each channel type with 0.5 Å bins. The center of mass (COM) of the total lipid is in green, the location of the nitrogen (N) is in blue, and the COM of the tails only (TAIL) is in black. RDFs are normalized by the expected bulk concentration per radial bin: $g(r) = \rho(r)/\rho_{\mathrm{bulk}}$.

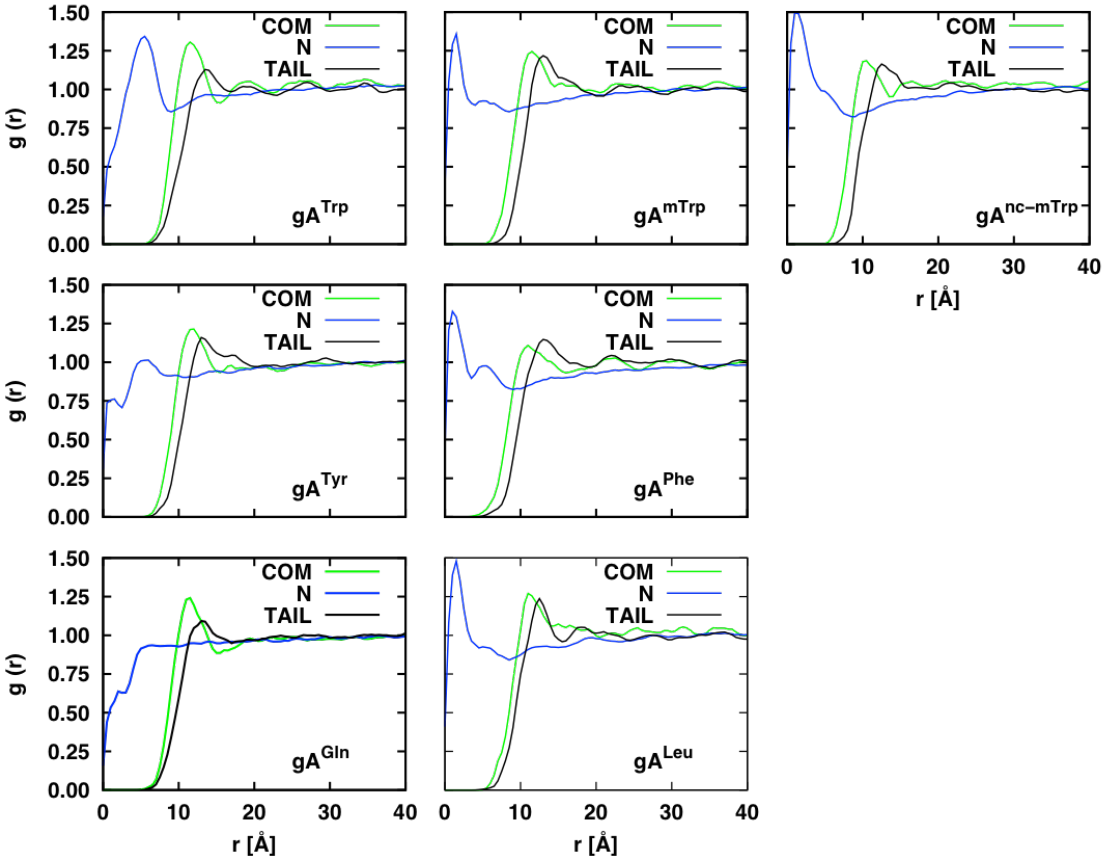

Figure S9. Contact plots between residue side chain heavy atoms and surrounding environments for each channel type in $dC_{18:1}$. The sum of the frequencies of the considered interactions is normalized to 1.0 for each residue.

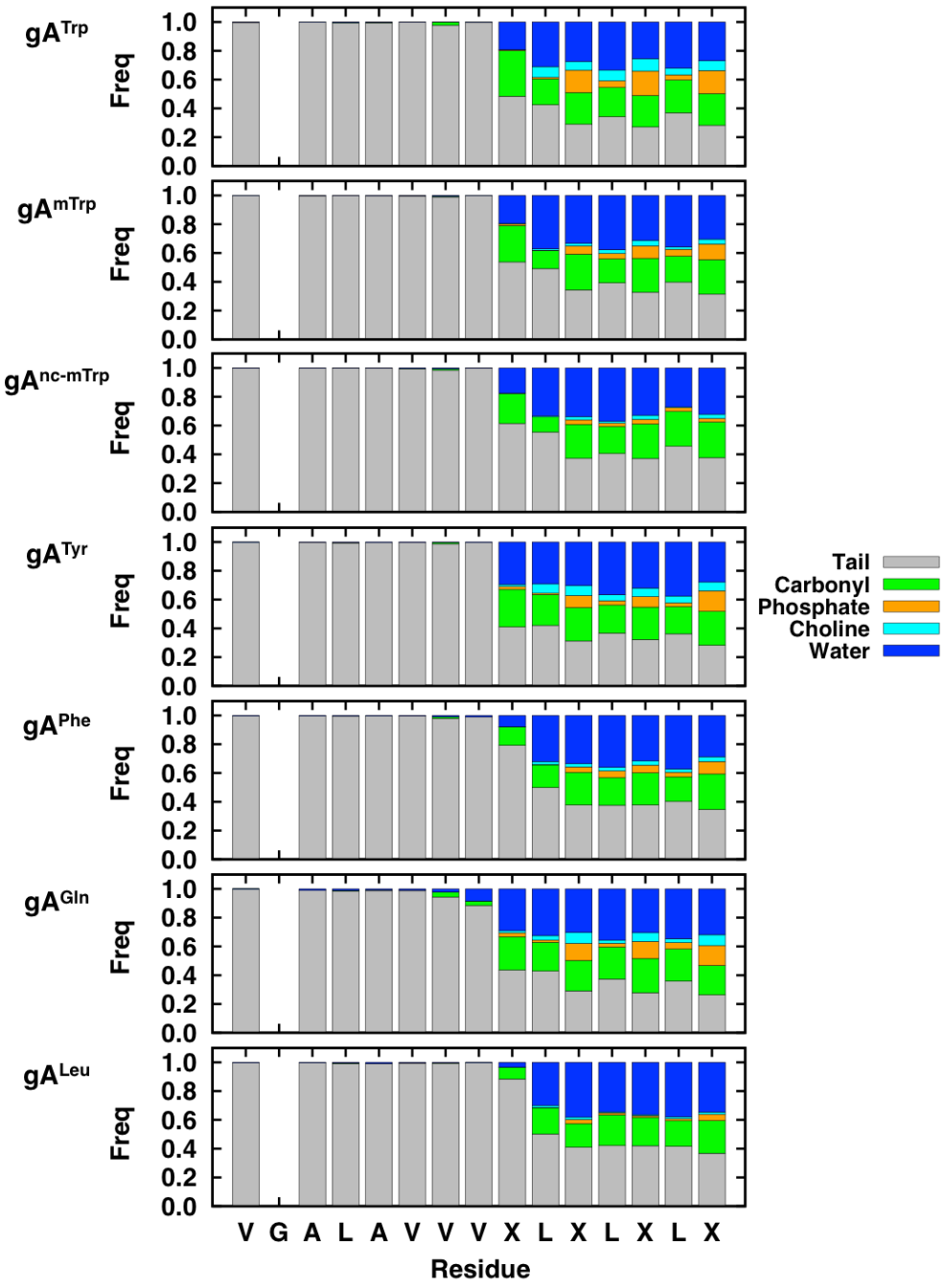

Figure S10. Trp χ_1-χ_2 dihedral angles in $dC_{18:1}$. Since it has been shown that backbone restraints (like dCMAP) affect residue dynamics, we compare (A) a previously published simulation[1] of gA^{Trp} in $dC_{18:1}$ using an RMSD backbone restraint (100 ns of sampling) to (B) a simulation from this study of gA^{Trp} in $dC_{18:1}$ using only dCMAP (600 ns of sampling). The RMSD restraint possibly reduces the dynamics of the Trp9 residue (it fluctuates around the initial χ_1-χ_2, which is the preferred orientation of this residue), whereas the dynamics of the other residues appear unchanged. The relative lack of sampling in the system with the RMSD restraint means that it is possible that simulation simply did not have enough time to sample other rotamer states. The true effect of a backbone restraint would have to be studied by a long timescale simulation, which is beyond the scope of this paper. Based on the χ_1-χ_2 plots, we conclude that while the backbone RMSD restraint might affect residue dynamics, it is likely minimal. See the **Figure S6** caption for the figure notation.

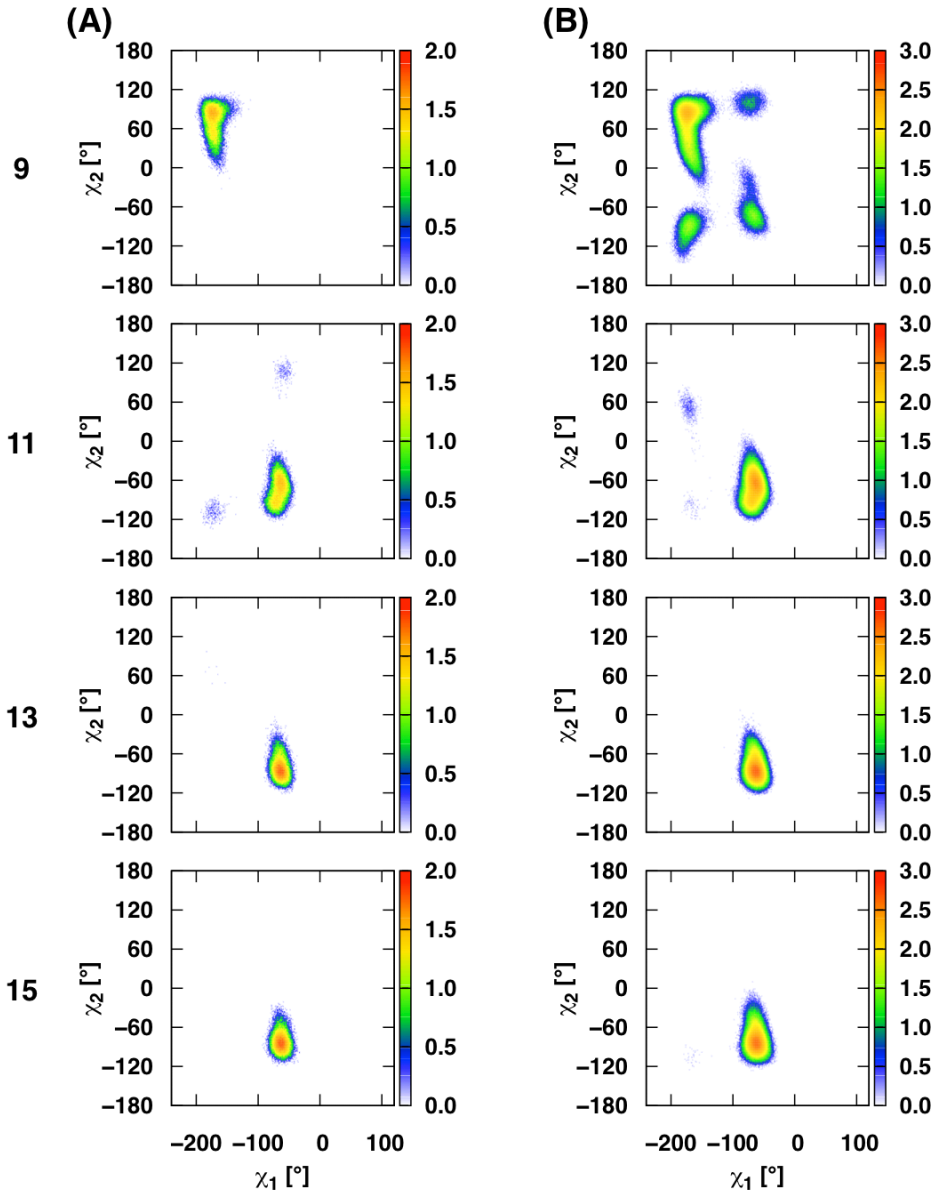

Figure S11. Heavy-atom *z*-density plots for the lipid C22 atom (black), entire channel (green), and the channel's interfacial residues (blue) in $dC_{20:1}$. Dotted red lines are shown to accentuate the entire channel peak shifts relative to gA^{Trp}. Data is plotted in 0.5 Å bins. Systems were centered by shifting the bilayer's center of mass to $z = 0$ Å.

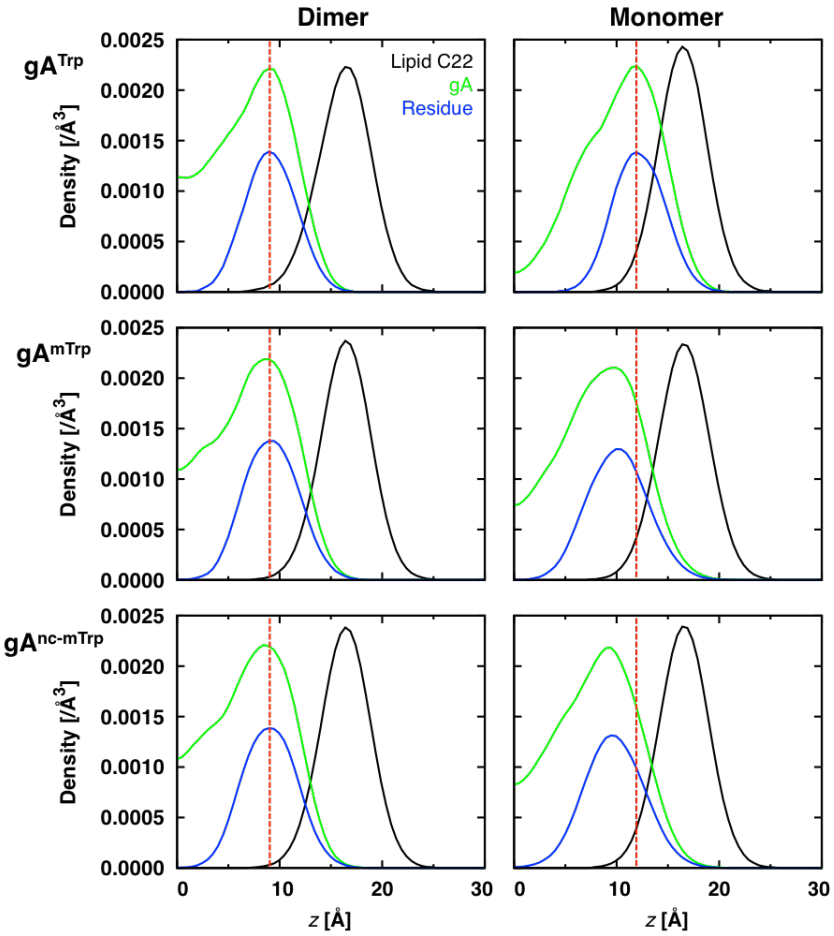

REFERENCES

(1) Sodt, A. J.; Beaven, A. H.; Andersen, O. S.; Im, W.; Pastor, R. W. Gramicidin A Channel Formation Induces Local Lipid Redistribution II: A 3D Continuum Elastic Model. *Biophys. J.* **2017**, *112* (6), 1198–1213.

(2) Kim, T.; Lee, K. Il; Morris, P.; Pastor, R. W.; Andersen, O. S.; Im, W. Influence of Hydrophobic Mismatch on Structures and Dynamics of Gramicidin A and Lipid Bilayers. *Biophys. J.* **2012**, *102* (7), 1551–1560.